

In-Situ FT-IRAS Study of the Hydrogenation of CO on Ru(001): Potassium-Promoted Synthesis of Formate

M. D. Weisel, J. L. Robbins, and F. M. Hoffmann*

Exxon Research and Engineering Company, Annandale, New Jersey 08801

Received: March 30, 1993; In Final Form: June 10, 1993*

Utilizing in-situ Fourier transform infrared reflection absorption spectroscopy, we have characterized potassium-promoted Ru(001) surfaces under CO hydrogenation conditions at elevated temperature and pressure (1–50 Torr). Interaction of the $\sqrt{3}\times\sqrt{3}$ -R30°-K-Ru(001) surface with CO at 300 K resulted in the formation of carbonate, which was hydrogenated to formate via the reaction $\text{K}_2\text{CO}_3 + \text{CO} + \text{H}_2 \rightleftharpoons 2\text{KHCO}_2$. The steady-state ratio of formate and carbonate coverage under reaction conditions was found to depend on the CO:H₂ pressure ratio, with carbonate being present in excess hydrogen. Time-resolved FT-IRAS determined the *initial* rate of formate synthesis from carbonate to $(1.7 \pm 0.8) \times 10^{-3}$ molecules site⁻¹ s⁻¹ at 500 K. Isotope transient measurements resulted in a comparable synthesis rate under *equilibrium* conditions and hence demonstrate the reactivity of the formate. The isotope transient data and the formate to carbonate conversion in excess hydrogen are consistent with two possible mechanisms: (i) Decomposition of the formate to carbonate, i.e., the reverse of the formate synthesis reaction, or (ii) further hydrogenation of the formate to methanol or methane. Characteristic vibrational features show that both formate and carbonate are *directly bound to the potassium*. This compound formation leads to a contraction of the potassium layer and to *island formation*. The formate observed under reaction conditions was shown to be more stable than model compounds produced under UHV conditions. This enhanced stability under reaction conditions is attributed to two factors: (i) The bond formation between potassium and the formate and (ii) physical site blocking due to coadsorbed CO. The results demonstrate a *dual promoter mechanism* of the potassium in the CO hydrogenation reaction over Ru(001)—(i) promotion of CO dissociation resulting in the formation of carbonate and (ii) direct participation of the potassium in the synthesis of formate via compound formation.

A. Introduction

The effect of alkali promoters in catalytic reactions has been the subject of intensive study due to their use in many important industrial processes, e.g., CO hydrogenation and methanol synthesis, coal gasification, and ammonia synthesis. Surface science studies have demonstrated that alkali additives alter the electronic structure of the underlying metal substrate.¹ This can modify the chemisorption bond of an adsorbed molecule and lead to *weakening of the bonds within the molecule*—thus promoting its dissociation. This effect is thought to be responsible for the promotional effect of potassium in the iron-catalyzed ammonia synthesis, where a lowering of the barrier for the dissociation of nitrogen is observed,² which results in a substantial increase in catalytic activity.³ A quite different effect of alkali promoters is their participation in the reaction. Alkali metals are highly reactive and tend to form compounds with most (oxygen-containing) molecules. The reactivity of the alkali atom with coadsorbed molecules is a strong function of alkali coverage and usually dominates at high alkali coverage, i.e., near saturation of the first layer, where the alkali atom exhibits “metallic” behavior.⁴ Both effects, electronic substrate modification and alkali compound formation, reveal an extremely complex behavior both with respect to the alkali coverage *and* the presence of other coadsorbates. These complexities have in many cases frustrated attempts to unambiguously characterize the role of alkali promoters in catalytic reactions. With the possible exception of the ammonia synthesis reaction, the mechanism of alkali promotion remains a subject of controversy.

One particularly interesting and important case is the CO hydrogenation reaction where alkali promoters exhibit different behavior for different metals. For transition-metal catalysts, e.g., Fe and Ni, the addition of an alkali promoter does not result in

an overall increase in the CO turnover rate (activity). Instead, alkali modifiers improve the selectivity toward more desirable products (higher hydrocarbons, olefins, oxygenates) at the expense of methane.^{5–8} Campbell and Goodman⁷ attributed the change in selectivity toward higher hydrocarbons to an increase in the steady-state level of active carbon, which is seen as a factor leading to increased C–C bond formation. While this model is helpful in explaining the increased C–C bond formation, it is *not necessarily the sole mechanism* responsible for the effect of alkalis on the selectivity in this reaction. For example, an important secondary reaction in Fischer–Tropsch chemistry is the readorption and incorporation of the primary products, alkenes. It is possible that potassium may modify either the adsorption of these alkenes or their hydrogenability to alkanes.⁸ Similarly, the improved selectivity toward oxygenates that is observed on Fe⁸ most likely results from changes in the surface chemistry of the alkali-promoted surface. An entirely different promotional effect is observed for copper where the CO hydrogenation activity/selectivity to methanol and higher alcohols is reported to increase on alkali-modified catalysts.^{9,10} In the case of methanol synthesis it is assumed that *CO reacts directly* (nondissociatively) to methanol through a formate intermediate. Formate can result from the reaction of the alkali hydroxide (CsOH or KOH) with carbon monoxide $\text{CO} + \text{OH}^- \rightarrow \text{HCOO}^-$.^{9,10}

In the present work we apply in-situ Fourier transform infrared reflection absorption spectroscopy (FT-IRAS) to characterize the state of potassium under CO hydrogenation reaction conditions over a Ru(001) surface. The use of FT-IRAS in combination with a single-crystal model catalyst has several advantages. FT-IRAS is an optical spectroscopy so we can access a large pressure range from 10⁻¹⁰ Torr to 1 atm. This enables us to prepare and characterize K–Ru surfaces using surface-sensitive probes under UHV conditions and then follow the reaction with in-situ FT-IRAS at elevated pressure and temperature, i.e., under catalytic reaction conditions (500–600 K, 1–100 Torr). The in-situ

* Abstract published in *Advance ACS Abstracts*, August 15, 1993.

capability is in this instance of particular importance, since the state of the alkali promoter is determined by the presence of the reactant gases and strongly depends on the pressure and temperature conditions during reaction. The use of a single-crystal model catalyst and the absence of a support material (SiO_2 , Al_2O_3) eliminates ambiguities about adsorbed species or reactions on the support. It further allows us to use infrared reflection spectroscopy, which provides full access to the spectral range from 4000 to 600 cm^{-1} without interference from optical absorption in the support material. The latter is particularly important both for the identification of alkali compounds and for the detection of adsorbed CO, since both have vibrational bands below the IR transmission cutoff of commonly used support materials.

B. Experimental Section

The experiments reported here were performed in a combined UHV/high-pressure reactor system.^{11,12} The multilevel UHV chamber (10^{-11} -Torr range) has been equipped for Fourier transform infrared reflection absorption spectroscopy (FT-IRAS), low-energy electron diffraction (LEED), Auger electron spectroscopy (AES), and thermal desorption mass spectroscopy (TDMS). The high-pressure reactor can be isolated from the UHV chamber with a gate valve allowing control of the gas pressure from 10^{-10} Torr to 1 atm. FT-IRAS was performed at the high-pressure reactor level, permitting both in-situ spectroscopy during reaction and ex-situ characterization of the surface after thermal quenching of the reaction and evacuation of the high-pressure cell. Infrared spectra were obtained in the single reflection mode at an 80° angle of incidence with a rapid-scanning Perkin-Elmer 1800 FTIR. Typically, vibrational spectra were obtained at 4-cm^{-1} resolution in the $4000\text{--}600\text{-cm}^{-1}$ range by averaging 200 scans in a total measurement time of 60 s. Time-resolved measurements were performed by averaging 16 scans at 4-cm^{-1} resolution with a duty cycle of 22 s. This mode permitted us to monitor the reaction by display of the vibrational spectra at 22-s intervals. (A faster time-resolved mode, which collects single scans in 300 ms, was not utilized in the present study, since it did not allow spectral display in real time.)

The Ru(001) sample (12-mm diameter) was cleaned and characterized for surface cleanliness according to procedures described elsewhere in detail.¹³ Potassium films were prepared by evaporation from a SAES getter source on both sides of the Ru(001) crystal. Procedures for preparing and characterizing the surface coverage and cleanliness of the potassium overlayer have been described in detail earlier.¹⁴ As observed in earlier work, the preparation of *clean* potassium films constituted a nontrivial problem and, therefore, particular attention was given to cleanliness tests at frequent intervals. As discussed elsewhere in detail,¹⁵ the contamination level determined from TDMS was found to be $\approx 0.3\%$ for CO (the major contaminant), which corresponds to a coverage of $\theta_{\text{CO}} \approx 0.001$ for a monolayer of potassium ($\theta_{\text{K}} = 0.33$). The amounts of other impurities (H_2 , CO_2 , and H_2O) were found to be smaller by at least 1 order of magnitude and thus just barely above the detection limit. For these experiments, a potassium coverage of $\theta_{\text{K}} = 0.33$ was chosen. This corresponds to the saturated monolayer and is characterized by a $\sqrt{3}\times\sqrt{3}\text{-R}30^\circ$ pattern in LEED.¹⁴

A typical experiment was performed in the following manner. After the Ru(001) was cleaned and the potassium film was prepared, the sample was translated to the high-pressure reactor level. Then the surface was exposed to 10^{-8} Torr of CO (with the gate valve open) in order to saturate the surface with a CO layer. After increasing the CO pressure to $>10^{-7}$ Torr, the high-pressure cell ($\approx 1000\text{-cm}^3$ volume) was isolated from the UHV chamber and then further pressurized with CO and H_2 to the desired reaction conditions. Both reactant gases were of research grade purity. However, CO was further purified by flowing the

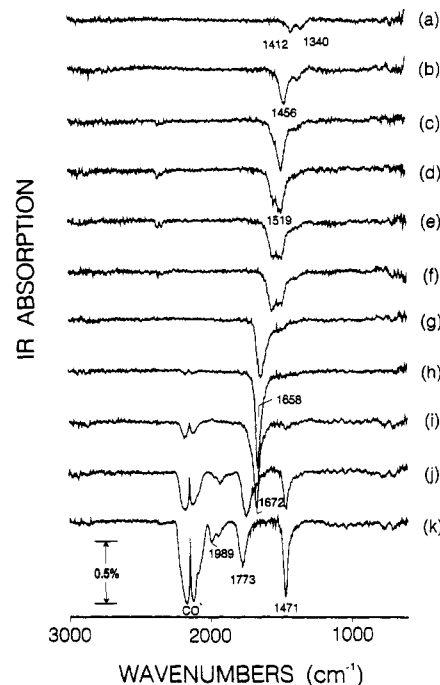


Figure 1. Vibrational spectra of CO adsorbed on a $\sqrt{3}\times\sqrt{3}\text{-R}30^\circ\text{-K-Ru(001)}$ surface at 300 K: (a)–(f) 2.5–15 langmuirs; (g) 2×10^{-6} Torr; (h) 2×10^{-3} Torr; (i) 2×10^{-2} Torr; (j) 2×10^{-1} Torr; (k) 2 Torr. The band labeled (CO*) is due to the gas-phase contribution of CO present in the reactor.

gas through a liquid nitrogen trap to remove residual carbonyls (particularly $\text{Ni}(\text{CO})_4$). Reaction products were measured either with a gas chromatograph (HP 5880A) or by following the evolution of the gas-phase bands with FTIR (e.g., CH_4) or with a differentially pumped mass spectrometer (located in the UHV chamber). The latter was also used to analyze the purity of the reaction gas. Turnover frequencies (TOF) are given as molecules/(site s), i.e., on a per Ru metal basis of the Ru(001) substrate (1.58×10^{15} atoms/ cm^2).

Following the high-pressure IR experiments, the sample was cooled to room temperature and then evacuated to 10^{-10} Torr (typically in 1–2 min). At each of these postreaction stages, infrared spectra were obtained to characterize changes in the surface due to quenching and evacuation. After the crystal was reintroduced into the UHV chamber, postreaction spectroscopies (TDMS, AES, LEED) were performed to characterize the state of the surface after reaction. Thermal desorption data were obtained with a UTI 100C mass spectrometer, which was enclosed in a stainless shield with a drift tube (5-mm diameter and 40-mm length) positioned 5 mm in front of the crystal. The mass spectrometer was interfaced to a PC-based data acquisition station (Teknivent Vector II), which allowed us to collect up to 15 masses every 0.5 s. The relative sensitivities of the various masses were calibrated to CO (1.0), CO_2 (1.25), H (0.3), H_2O (≈ 0.05 for KOH), and K (0.010), as described elsewhere in detail.¹⁵

C. Results and Discussion

The experimental results are described in two sections. In the first section we characterize the state of the potassium promoter and the adsorbates observed under CO/ H_2 reaction conditions. In the second section we investigate the reactivity of the observed surface species and compare their stability and thermal decomposition behavior with that of model compounds synthesized under UHV conditions.

I. Alkali Promoter States and Characterization of Reaction Intermediates. Experimental results characterizing the reaction of CO and H_2 with a potassium-promoted Ru(001) are shown in Figures 1 and 2. The vibrational spectra shown in Figure 1

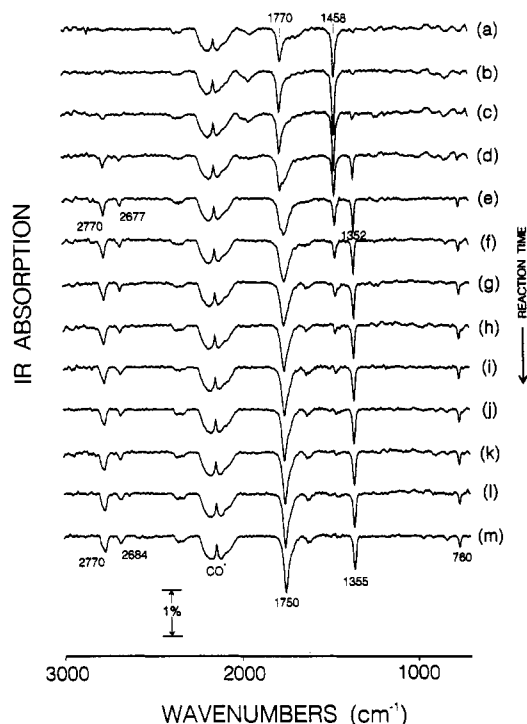


Figure 2. Vibrational spectra obtained during the CO/H₂ reaction over a $\sqrt{3}\times\sqrt{3}$ -R30°-K-Ru(001) at 500 K (1 Torr of CO + 2 Torr of H₂). The time interval between the spectra was 74 s. The band labelled (CO*) is due to the gas-phase contribution of CO present in the reactor.

were obtained after preparing a $\sqrt{3}\times\sqrt{3}$ -R30°-K-Ru(001) surface ($\theta_K = 0.33$) under UHV conditions and subsequent exposure to CO at 300 K. Initially, after an exposure of 2.5 langmuirs, two weak bands appear at 1340 and 1412 cm⁻¹ (a). With increasing exposure a broad band evolves, which increases in intensity and shifts to higher frequency (b–i). This band saturates at a CO equilibrium pressure of 0.02 Torr at 1672 cm⁻¹ (i). At this pressure an additional broad band at 2143 cm⁻¹ appears which is due to gas-phase CO in the reactor cell.¹⁶ Further increase in CO pressure to 0.2 Torr results in a splitting of the 1672-cm⁻¹ band into two bands at 1468 cm⁻¹ and 1740 cm⁻¹ (j). These bands shift in frequency to 1471 and 1773 cm⁻¹ upon further increase in CO pressure to 2 Torr (k). The lower frequency band also increases further in intensity. Heating to 500 K, the reaction temperature of Figure 2, causes no major changes in the vibrational spectra except for a further increase in intensity of the bands at 1773 and 1471 cm⁻¹.

The vibrational spectra in Figure 1a–i are characteristic for CO adsorbed in the presence of a $\sqrt{3}\times\sqrt{3}$ -R30°-K layer on the Ru(001) surface. In earlier work utilizing EELS,¹⁷ CO adsorption on this surface at 80 K was found to result in two bands at 1370 and 1490 cm⁻¹, the former band (1370 cm⁻¹) dominating at low exposure (1 langmuir) and the latter (1490 cm⁻¹) at higher exposures (5 langmuirs). On the basis of isotopic substitution with ¹³C¹⁸O, both bands were attributed to C–O stretching vibrations of adsorbed CO. Thermal desorption data further indicated that for the potassium-modified Ru(001) surface the sticking coefficient for CO was strongly reduced by a factor of 5–10 due to physical site blocking by the potassium atoms.¹⁷ The latter is consistent with the unusually high exposure needed to saturate the surface with adsorbed CO (Figure 1a–f). The frequency shift of this band with increasing CO coverage has also been observed in earlier work.¹⁴ At higher CO pressures spectra (j) and (k) characterize a distinctly different adsorbate layer. There, the band at 1672 cm⁻¹ in spectrum (i) has been replaced by two bands, at a lower (1471 cm⁻¹) and a higher frequency (1773 cm⁻¹). Additional weak bands are found at 1900–2000 cm⁻¹. These are due to CO adsorption on parts of the ruthenium substrate that are only weakly modified by potassium,¹⁴ indicating

a contraction of the potassium layer. This observation, combined with the peak splitting, suggests compound formation with the potassium atoms. Based on a UHV model study using FT-IRAS and photoemission, we assign the band at 1471 cm⁻¹ to potassium carbonate. In this study, the interaction of CO₂ with a $\sqrt{3}\times\sqrt{3}$ -R30°-K-Ru(001) surface resulted in a similar vibrational band at 1460 cm⁻¹,¹⁸ and a valence band photoemission spectrum characteristic of carbonate.¹⁹ Similar vibrational bands have also been observed after the interaction of CO₂ with potassium or sodium over Al(100),²⁰ Fe(100),²¹ Pt(111),²² and Pd(111)²³ and for bulk carbonate.²⁴ The band at 1773 cm⁻¹ in spectrum (k) is assigned to CO adsorbed on Ru next to the potassium carbonate. In making the above assignments we are aware of the complexity of assigning vibrational frequencies in this spectral range. Previous work has shown that CO adsorbed in the presence of potassium can exhibit a C–O stretching vibration ranging from 1300 to 2000 cm⁻¹ depending on the respective K and CO coverages.¹⁴ However, the fact that the band at 1471 cm⁻¹ is affected by hydrogenation and the band at 1773 cm⁻¹ is not (discussed below) supports the assignment of the former to a carbonate species and the latter to CO coadsorbed on the ruthenium substrate.

The spectra in Figure 1 show that CO reacts with K/Ru(001) to form potassium carbonate (K₂CO₃) at 300 K in moderate pressure of CO (0.02–2 Torr). This reaction formally involves oxidation of potassium and CO by one and two electrons, respectively. Carbon monoxide is the only available oxidant in this system. It can effectively serve as an oxidant via CO disproportionation (reaction 1) or by CO dissociation (reaction 2), which is considered as one of the steps involved in CO disproportionation.



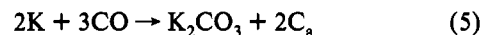
In reaction 2 it is likely that the surface oxygen is associated with the most electropositive surface component, potassium:



Alkali oxides react readily with CO₂ to form alkali carbonates, which are stable materials up to very high temperatures:



The sum of reactions 1–4 may account for the net chemistry seen here:



The formation of potassium carbonate is well documented by the observed IR vibrational spectra and photoemission valence band data. There is a substantial contraction of potassium as it converts from the metallic form in the bulk with a K–K distance of 4.51 Å²⁵ to ionic K⁺ with a K–K distance of 3.45 Å in carbonate²⁶ and 3.51 Å in formate.²⁷ The contraction of the potassium layer, which has in the $\sqrt{3}\times\sqrt{3}$ -R30°-K layer a metal like K–K distance of 4.5 Å, is indicated by the simultaneous appearance of adsorbed CO, which is only weakly modified by potassium ($\nu_{\text{CO}} \approx 1990$ cm⁻¹) in Figure 1. A similar contraction of the $\sqrt{3}\times\sqrt{3}$ -R30°-K-Ru(001) layer following compound formation has been reported for potassium formate where a contraction of the potassium layer by about 20% was observed.¹⁵ Finally it is worth noting that the conversion of CO to carbonate requires only moderate reaction temperatures (300 K) in the presence of potassium. This is a clear indication that *the dissociation of CO is promoted by the presence of potassium*. In the absence of potassium, the dissociation of CO on Ru(001) is negligible at low pressure and proceeds at significant rates only at elevated pressures (>10⁻⁴ Torr) and reaction temperatures (>600 K).¹² The surface carbon anticipated from reaction 5 could be responsible for the appearance of vibrational bands at 700–800 cm⁻¹ in Figure 1i–k. However,

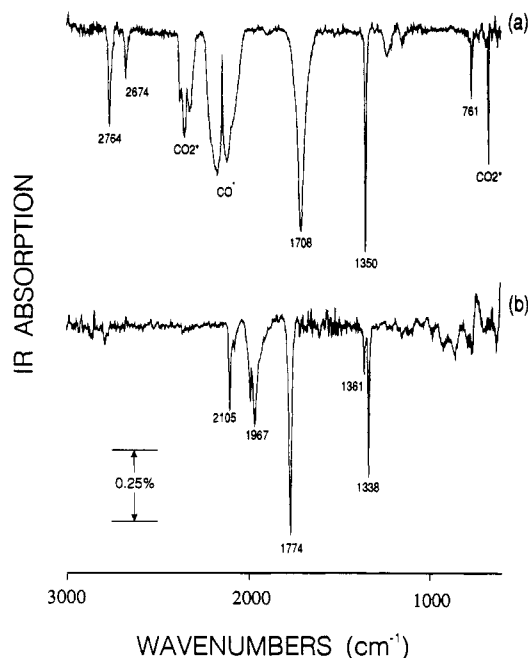


Figure 3. Vibrational spectra of reaction intermediate observed during CO/H₂ reactions over K-Ru(001) (a) and after a H₂ → D₂ isotope switch followed by evacuation (b).

no conclusive identification was made due to possible IR background drifts at elevated temperature and pressure, which prevented us from assigning weak, broad bands with confidence in the spectral range below 800 cm⁻¹.

The effects of hydrogen addition are shown in Figure 2 with time-resolved vibrational spectra. The sequence was obtained after preparing a K-Ru surface in 1 Torr of CO under similar conditions as in Figure 1k, and subsequent heating to 500 K. Spectrum (a) in Figure 2 shows the two characteristic bands at 1458 cm⁻¹ and 1770 cm⁻¹ observed earlier. Sequence (a)–(k) displays the effect of the addition of 2 Torr of H₂ at 500 K as a function of reaction time. The band at 1458 cm⁻¹ decreases, while at the same time several new bands appear at 2770, 2677, 1352, and 760 cm⁻¹. Interestingly, the band at 1770 cm⁻¹ does not change much with time except for a small shift to lower frequency, (c)–(f). After the new features saturate in intensity, no further changes occur with increasing reaction time. The new bands observed in H₂/CO at 2770, 2677, 1352, and 760 cm⁻¹ suggest the synthesis of surface formate. Isotope substitution experiments and model compound studies support this assignment. Figure 3 demonstrates the effect of an isotope switch in the reactant gas from H₂ to D₂. Spectrum (a) shows the spectrum obtained during reaction at 500 K in CO/H₂, while spectrum (b) was obtained after switching the reactant gas to CO/D₂. Gas-phase CO obscures the C–D stretching region, so spectrum (b) was recorded after cooling the crystal to 300 K and evacuating the reactor. We recognize the characteristic isotopic shift of the C–H stretching mode from 2764 cm⁻¹ to 2105 cm⁻¹. On the other hand, the mode at 1350 cm⁻¹ in (a) exhibits no significant shift with isotopic substitution, indicating that it is largely a C–O vibration. This suggests a formate species as shown by comparison with data from model compounds presented in Figure 4 and Table I. In Figure 4 we compare vibrational spectra of the surface species observed during reaction (spectrum (a)) with various formate species prepared under UHV conditions (spectra (b)–(d)). Spectrum (b) shows a monolayer of potassium formate produced from the decomposition of formic acid on a $\sqrt{3}\times\sqrt{3}$ -R30°-K-Ru(001) layer.^{15,28} Spectrum (c) represents bulk potassium formate produced from the decomposition of formic acid on a potassium multilayer on Ru(001), while spectrum (d) shows a formate layer adsorbed in the absence of potassium on clean Ru(001). The assignment of the vibrational bands in spectra

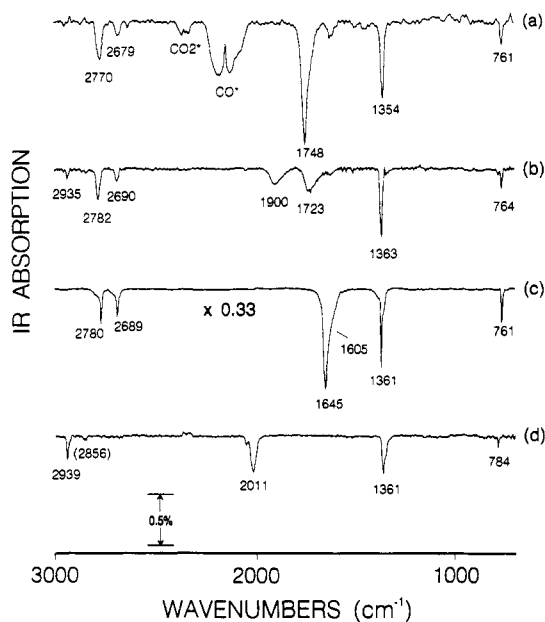


Figure 4. Vibrational spectra of various formate species observed on Ru(001) surfaces: (a) reaction intermediate observed during CO/H₂ reaction of K-Ru(001); (b) potassium formate monolayer on Ru(001); (c) bulk potassium formate on Ru(001); (d) formate monolayer adsorbed on clean Ru(001).

(b)–(d) has been discussed in detail elsewhere.¹⁵ The good agreement between the spectra (a)–(c) shows that the observed species in (a) must be potassium formate. Therefore, we are able to assign the vibrational bands of the observed reaction intermediate in spectrum (a) at 2770 cm⁻¹ to the C–H stretch $\nu(\text{CH})$, at 1354 cm⁻¹ to the symmetric C–O stretch $\nu_s(\text{OCO})$, and at 761 cm⁻¹ to the CO deformation mode $\delta(\text{OCO})$. The band at 2679 cm⁻¹ is assigned to a Fermi resonance of the overtone of the C–H bending mode with the C–H stretch at 2770 cm⁻¹ based on isotopic substitution spectra discussed elsewhere.¹⁵ As shown in Table I, the vibrational bands are also in good agreement with literature data for bulk potassium formate reported by Ito and Bernstein,²⁹ for surface formate adsorbed on K–Al₂O₃ by Kantschewa et al.,³⁰ and on Cs/Cu/ZnO catalysts by Klier et al.⁹ Figure 4 and Table I further demonstrate that the formate species observed during reaction is bound to potassium and not to the ruthenium substrate. Formate bound to potassium exhibits characteristic frequency shifts for the C–H stretch $\nu(\text{C–H})$ and in the bending mode $\delta(\text{OCO})$ in comparison to formate bound to ruthenium. Figure 4d shows a formate species bound to the ruthenium substrate with $\nu(\text{CH})$ at 2939 cm⁻¹ and $\delta(\text{OCO})$ at 784 cm⁻¹. In comparison, for potassium formate (Figure 4a,b), both the C–H stretch and the CO deformation modes are shifted to higher frequency by 140 and 20 cm⁻¹, respectively. These characteristic frequency shifts, and the good agreement with bulk potassium formate (c), are clear evidence that *the formate observed during reaction is bound to potassium and not to the ruthenium substrate*. The spectrum of the potassium formate monolayer in Figure 4b shows both potassium- and ruthenium-bound formate present at the surface. In addition to the potassium formate features at 2782, 2690, 1363, and 764 cm⁻¹, we also find a small amount of formate adsorbed to the ruthenium substrate as evidenced by weak bands at 2935 and 784 cm⁻¹. The appearance of the latter bands suggests the presence of potassium-free ruthenium domains, which must be due to a contraction of the K-layer resulting from compound formation. For the pure potassium layer on Ru(001) no evidence of island formation has been observed due to the strong K–K repulsion for potassium coverages $\theta_K > 0.05$.¹⁴

Remarkable in the “monolayer” formate spectra (Figure 4a,b,d) is the absence of the asymmetric C–O stretching mode (≈ 1600 cm⁻¹). Therefore we can assign the symmetry of these surface

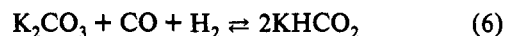
TABLE I: Vibrational Frequencies of Formate Species Adsorbed on Alkali-Promoted Surfaces (Top Panel) and on Unpromoted Metal Surfaces (Bottom)

C_{2v}	$\nu(\text{CH})$ A_1	$\nu_s(\text{COO})$ B_1	$\delta(\text{CH})$ B_1	$\nu_s(\text{COO})$ A_1	$\pi(\text{CH})$ B_2	$\delta(\text{COO})$ A_1	ref
K-Ru(001) (CO/H ₂)	2770	2679		1354		761	this work
K-Ru(001) monolayer from HCOOH	2782	2690		1363		764	15
K-Ru(001) multilayer from HCOOH	2780	2689	1645, 1605	1361		761	15
HCOO ⁻ K ⁺ (bulk)	2803	2728	1585	1351	1069	750	29
HCOO ⁻ /K-Al ₂ O ₃	2770		1590	1350			30
Cs/Cu/ZnO (CO/H ₂)	2753	2660					9
Cu/ZnO (CO/H ₂)	2928	2857					9
Au/ZrO ₂	2880	2750	1580, 1600	1360, 1380			31
Ru(001)	2939			1361		784	15

formate species to the C_{2v} point group, as discussed elsewhere in detail.¹⁵ As indicated in Table I, only modes that belong to the totally symmetric representation (A_1) are observed. B_1 or B_2 modes, e.g., the asymmetric C–O stretch (B_1), are not observed, in accordance with the surface dipole selection rule for C_{2v} . The latter mode is only observed in the spectrum of bulk KHCO₂ (Figure 4c) with a band at 1645 cm⁻¹. From the C_{2v} symmetry of the monolayer species we conclude that the two oxygen atoms are equivalent. From the good agreement for the vibrational frequencies of the formate modes observed in (a) and (b), we can suggest for the formate observed during reaction a similar bonding model as previously suggested for the potassium formate monolayer species on Ru(001).¹⁵ In this configuration, which is based on the structure of bulk potassium formate,³³ each oxygen is bound to two potassium atoms and each of the potassium atoms is bound to both oxygen atoms of the formate. Such a bonding configuration will also result in a contraction of the potassium layer, as discussed earlier.

The spectral sequence in Figure 2 shows that the formation of potassium formate coincides with the disappearance of the band at 1460 cm⁻¹, which was assigned to potassium carbonate earlier.¹⁸ It thus appears that carbonate is a precursor to formate, as discussed further below. On the other hand, the band at 1770 cm⁻¹ in Figure 2 is hardly affected by hydrogenation, suggesting that this band is not related to the carbonate but is rather due to CO adsorbed next to the potassium. The C–O stretch frequencies observed for coadsorbed CO in Figures 1 and 2 are consistent with the presence of the alkali in three states: elemental potassium, potassium carbonate, and potassium formate. Previous work has shown that the CO is a very sensitive molecular probe of the electronic substrate modification caused by potassium and hence a probe of the “ionicity” of the potassium species.¹⁴ The small frequency shift from 1770 to 1750 cm⁻¹ (Figure 2) then suggests that the reaction of potassium carbonate to formate has only a small effect on the “ionicity” of the potassium. In contrast, the transition from elemental potassium to carbonate in Figure 1 induces a much larger change in the “ionicity” resulting in a much larger C–O frequency shift from 1672 to 1773 cm⁻¹ (Figure 1j,k) of the coadsorbed CO molecule. Similar values of the CO stretch frequency (≈ 1750 cm⁻¹) have also been observed for CO coadsorbed with KOH and KO₂ species on Ru(001).³⁴

The conversion of potassium carbonate to potassium formate in the presence of H₂ and CO can be presented by reaction 6:



This reaction can be viewed as the sum of two simpler processes involving the reduction of potassium carbonate by hydrogen (reaction 7) and the production of formate by reaction of CO with potassium hydroxide intermediates (reaction 8):



This model, in particular reaction 7, is supported further by an experiment where a layer of potassium carbonate has been

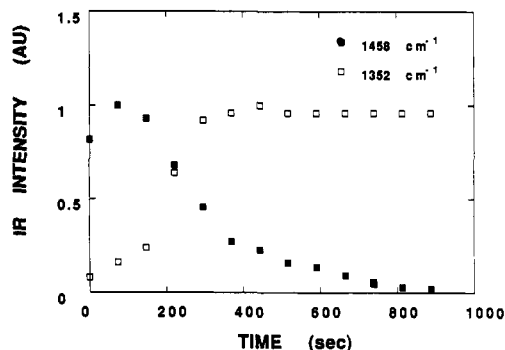


Figure 5. IR intensities of the formate band at 1352 cm⁻¹ (□) and the carbonate band at 1458 cm⁻¹ (■) plotted as a function of reaction time (see Figure 2).

produced by the interaction of CO₂ with a $\sqrt{3}\times\sqrt{3}$ -R30°-K-Ru(001) surface under UHV conditions via the reaction $2\text{K} + 2\text{CO}_2 \rightarrow \text{K}_2\text{CO}_3 + \text{CO}_a$. Subsequent reaction of this surface in 10 Torr of H₂ without added CO at 500 K results in a rapid conversion of the carbonate to formate (reaction 7).³⁵ Support for reaction 8 comes from the fact it provides a facile route to alkali formates at moderate temperatures.³⁶ This reaction has also been suggested as the pathway to formate intermediates in the methanol synthesis reaction over Cu/Cs/ZnO catalysts⁹ and in the water gas shift reaction over K-Al₂O₃ catalysts.³⁷ At low pressure (UHV) the reverse of reaction 8 is the dominant pathway for the decomposition of the potassium formate.¹⁵

II. Reactivity, Stability and Thermal Decomposition of the Formate. The observation of a formate species under CO hydrogenation conditions poses the important question of the further fate of the formate, i.e., whether it is a reactive intermediate participating in the formation of products or constitutes merely an unreactive “spectator”. Support-bound formate species have been observed previously during CO/H₂ reactions over supported metals, but there has been much controversy in the catalysis literature whether these species actually participate in the formation of reaction products such as methanol or merely constitute unreactive spectators adsorbed on the support.^{38–40} In the present case of an unsupported single-crystal metal surface we can obviously exclude adsorption on the support. In order to investigate the reactivity of the formate species and its thermal stability, we have performed a series of experiments that are presented in this section.

The Rate of Formate Synthesis. In order to estimate the synthesis rate of the formate from potassium carbonate, we present in Figure 5 a time-resolved plot characterizing the increase of formate as a function of reaction time after the introduction of hydrogen. The plot, which is based on the vibrational spectra shown earlier in Figure 2, shows the integrated IR intensities of the formate band at 1352 cm⁻¹ and the carbonate band at 1458 cm⁻¹ as a function of reaction time at 500 K and 1 Torr of CO + 2 Torr of H₂. The data confirm our earlier observation that the formation of the formate species occurs simultaneously with the disappearance of the carbonate species in agreement with

reaction 6. The integrated area of the IR band at 1352 cm^{-1} can be used to estimate the initial rate of formate synthesis at 500 K to $(1.7 \pm 0.8) \times 10^{-3}$ molecules/(sites). The absolute coverage was calibrated by comparison of the IR intensity of the formate band at 1352 cm^{-1} observed under reaction conditions with that of a potassium formate monolayer ($\theta = 0.33 \pm 0.05$) produced under UHV conditions (cf. Figure 4b).¹⁵ The large error margin in the rate comes largely from the uncertainty in the nonlinear coverage dependence of the IR intensity, which introduces an error in the coverage determined from IR intensities at *high* formate coverage.⁴¹ This nonlinearity is also evident from Figure 5, where saturation of the formate band is observed at 400 s while the carbonate band still has about 20% of its original intensity. It is important to note that the synthesis rate determined above represents a *nonequilibrium* case, since the formate was formed after introduction of the reactant (H_2) and not under equilibrium conditions of static pressure. Therefore this rate represents the synthesis of formate from carbonate at low formate coverage.

Isotope Transient Measurement. In order to determine the synthesis rate of formate under *equilibrium* conditions, i.e., at high formate coverage, we have performed isotopic transient measurements. In this case the equilibrium conditions of constant pressure and reaction temperature are maintained by replacing one of the reactants with its isotopic substitute and by following the appearance of the isotopic label in the intermediate or reaction product. Time-resolved vibrational spectra of an isotope switch experiment are shown in Figure 6. The spectra were obtained following the addition of 3 Torr of C^{18}O to a reaction gas consisting of 2.5 Torr of $\text{H}_2 + 2.5$ Torr of C^{16}O with the sample held at 450 K.⁴³ At time of the introduction of C^{18}O ($t = 0$), the surface is characterized by a layer of potassium formate ($\theta_{\text{HCOO}} \approx 0.30$), as evident from the formate band at 1351 cm^{-1} . Addition of the C^{18}O isotope to the reactor gas results in a decrease in the formate band at 1351 cm^{-1} and a simultaneous appearance of a band at 1327 cm^{-1} . This band can be assigned to partially labeled formate $\text{HC}^{16}\text{O}^{18}\text{O}$ on the basis of a comparison with theoretically predicted isotope shifts, shown at the bottom of Figure 6.⁴⁴ The band predicted for the fully labeled species $\text{HC}^{18}\text{O}^{18}\text{O}$ cannot be identified with confidence since its intensity is below the noise level. Figure 7 shows a plot of the integrated intensities of the bands at 1351 cm^{-1} (■) and 1327 cm^{-1} (□) versus reaction time. The dashed line shows the increase in the C^{18}O pressure measured by a differentially pumped mass spectrometer. The plot shows that the isotope label appears immediately in the formate and fully saturates in intensity after a reaction time of approximately 50 s. From the initial rise of the $\text{HC}^{16}\text{O}^{18}\text{O}$ band, we estimate a formate synthesis rate of $3.3 \pm 1.5 \times 10^{-3}$ molecules/(site s). The ratio of the IR band intensities $\text{HC}^{16}\text{O}^{16}\text{O}:\text{HC}^{16}\text{O}^{18}\text{O}:\text{HC}^{18}\text{O}^{18}\text{O}$ is found to be 1:0.7:0.2. For complete scrambling the intensity ratio is predicted to be 1:2:1 for equal pressures of C^{16}O and C^{18}O . This apparent discrepancy, however, does not necessarily reflect incomplete isotopic scrambling. It is actually expected from vibrational coupling of two dipoles vibrating with different frequencies, which will lead to intensity transfer from the low-frequency to the high-frequency band. This intensity transfer, which is a measure of the intermolecular distance, can be considerable if the frequencies are close, as in the present case. For a comparable case, $\text{CO}/\text{Pd}(100)$ with an 1:1 isotopic mixture of ^{12}CO and ^{13}CO ($\theta_{\text{CO}} \approx 0.5$), two IR bands were observed with an intensity ratio of 4:1.⁴² Therefore, in the present case, the observation of a nonstoichiometric ratio of the IR band intensities is not surprising and indicates the vibrational coupling between neighboring molecules. This conclusion agrees with our earlier observation of a contraction of the potassium layer, which results in a smaller intermolecular distance between two neighboring formate molecules (approximately 3.5 \AA).¹⁵

There are two possible mechanisms to account for the isotopic transient data. First, *hydrogenation of the formate* to products

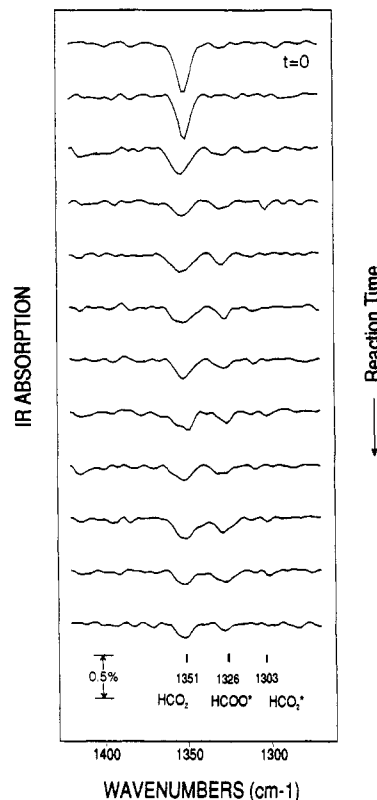


Figure 6. Isotopic substitution spectra obtained after introduction of 3 Torr of C^{18}O in addition to 5 Torr of CO/H_2 (1:1) at 450 K. The spectra are shown as a function of increasing reaction time at intervals of 22 s. The vertical lines at the bottom of the panel indicate the position of the various isotopic labels predicted from calculations.

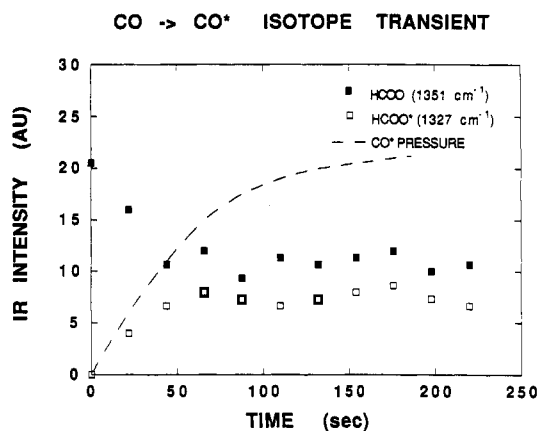


Figure 7. IR intensities of the symmetric CO stretch of HCO_2 at 1351 cm^{-1} (■) and for HCO^{18}O at 1327 cm^{-1} (□) as a function of reaction time. The dashed line shows the increase of the C^{18}O pressure in the reactor as measured by a differentially pumped mass spectrometer.

and, second, *decomposition of the formate* involving an equilibrium between the formation and decomposition of the formate. Both mechanisms are discussed further below. An alternative *direct scrambling mechanism*, which does not involve C–O bond breaking of the formate, can be excluded. Such a direct isotopic exchange involving tunneling has been frequently proposed for $\text{D} \rightarrow \text{H}$ exchange, but to our knowledge there is no example of such a mechanism involving isotopes of oxygen or carbon.

Reaction in Hydrogen. Figure 8 shows vibrational spectra obtained after switching from a CO/H_2 to a pure H_2 atmosphere. Spectrum (a) characterizes the surface after reaction at 475 K in a CO/H_2 atmosphere (and subsequent quenching to 300 K) with formate bands at 2781 and 1362 cm^{-1} . Evacuation to $\approx 10^{-2}$ Torr (spectrum (b)), introduction of 0.5 Torr of hydrogen (spectrum (c)), and heating of the surface to 380 K result in the

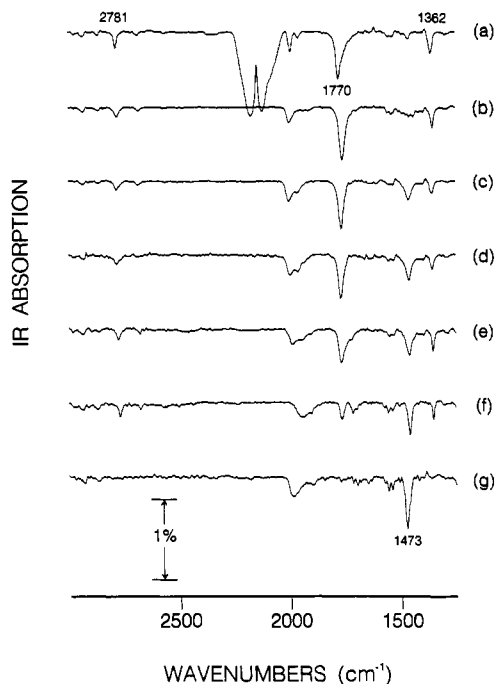


Figure 8. Reactivity of the formate in pure hydrogen. (a) 3 Torr of CO + 1 Torr of H₂, 300 K; (b) evacuation to 10⁻² Torr; (c) 0.5 Torr of H₂, 300 K; (d) 320 K; (e) 340 K; (f) 360 K; (g) 380 K.

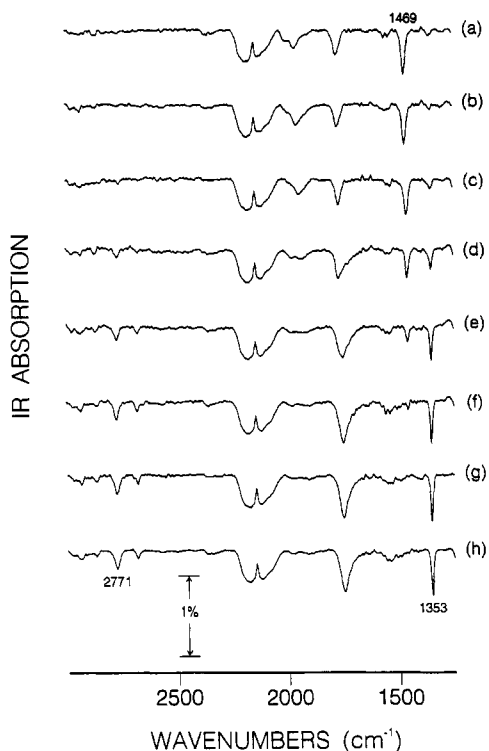


Figure 9. Reintroduction of CO results in the reappearance of the formate. (a) 0.5 Torr of H₂ + 0.5 Torr of CO, 360 K; (b) 380 K; (c) 400 K; (d)-(h) 420 K, increasing reaction time in 45-s increments.

disappearance of the formate bands. The latter are replaced by a carbonate band at 1473 cm⁻¹ (spectra (d)-(g)). The reverse effect, i.e., reappearance of the formate upon reintroduction of the CO, is demonstrated in Figure 9. Addition of 0.5 Torr of CO to the H₂ (0.5 Torr) and subsequent heating to 420 K (spectra (a)-(d)) results in the reappearance of the vibrational features of formate, (d)-(h). The spectra in Figures 8 and 9 suggest that formate and carbonate are interconvertible and that their relative populations depend on the relative (and total) pressure of H₂ and CO. The latter effect has been explored in more detail in an experiment where the partial pressures of H₂ and CO have been

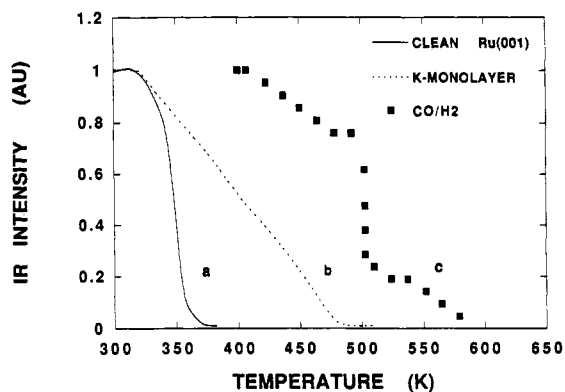


Figure 10. Comparison of the thermal stability of different formates shown as a plot of the IR intensity of the symmetric CO stretch at 1350 cm⁻¹ as a function of temperature: (a) formate adsorbed on *clean* Ru(001) (solid line); (b) potassium formate monolayer on Ru(001) (dashed line); (c) potassium formate produced during reaction in 10 Torr CO + 40 Torr H₂ on a $\sqrt{3}\times\sqrt{3}$ -R30°-K-Ru(001) surface (■). Heating rates: (a) 0.5 K/s; (b) 1 K/s; (c) 0.2 K/s (see text for details).

alternatively increased (not shown here). Thus, excess hydrogen (CO:H₂ ratio of 1:10) resulted in the conversion of formate to carbonate, while the addition of CO to a more moderate CO:H₂ ratio of 1:2 converted the carbonate back to formate.⁴⁵

The data presented in Figure 8 are remarkable since they demonstrate the high reactivity of the formate in hydrogen under mild conditions (380 K). It is interesting to note that in all cases the conversion from formate to carbonate is accompanied by the disappearance of the CO band at 1750 cm⁻¹. The latter band has been previously assigned to CO adsorbed in the vicinity of potassium. On the other hand, the reappearance of the formate, e.g., in Figure 9, is accompanied by the appearance of this band. This suggests that coadsorbed CO could play an important role in stabilizing the potassium formate on the surface. The removal of this CO species by the reaction with hydrogen (Figure 8) then might be responsible for the increased reactivity (decomposition) of the formate.

Thermal Stability and Decomposition of the Formate. The thermal stability of formate formed under reaction conditions is demonstrated in Figure 10, which shows a plot of the IR intensity of various formate species (1360-cm⁻¹ band) as a function of reaction temperature. Curve (c) shows the thermal stability of the formate layer produced at 400 K in 10 Torr of CO + 40 Torr of H₂. The reaction temperature was increased in steps from 400 to 500 K at a heating rate of 0.2 K/s, followed by isothermal heating for 28 min at 500 K and further heating from 500 to 600 K at 0.2 K/s until all of the formate had disappeared.⁴⁶ The thermal stability of the formate under high-pressure conditions is remarkable in comparison to formate model compounds studied under UHV conditions.¹⁵ A formate layer produced from the decomposition of formic acid on potassium-free "clean" Ru(001) (as in Figure 4d) fully decomposes by 350 K (solid line). The potassium formate monolayer produced from the decomposition of formic acid on $\sqrt{3}\times\sqrt{3}$ -R30°-K-Ru(001) (as in Figure 4b) is more stable, but its decomposition is complete at 480 K (dashed line). The data demonstrate that the increase in thermal stability of the potassium formate observed under reaction conditions must be due to two factors. First, compound formation of the formate with potassium is important and contributes to the thermal stability as evident from the comparison between curves (a) and (b). Second, it appears that the effect of the high-pressure environment results in the presence of coadsorbed CO at elevated temperature, which provides additional thermal stability of the formate.

The postreaction thermal desorption spectra, shown in Figure 11, characterize both the thermal decomposition of the formate and the thermal stability of the potassium layer. The spectra were obtained after reaction of 2 Torr of CO + 13 Torr of H₂

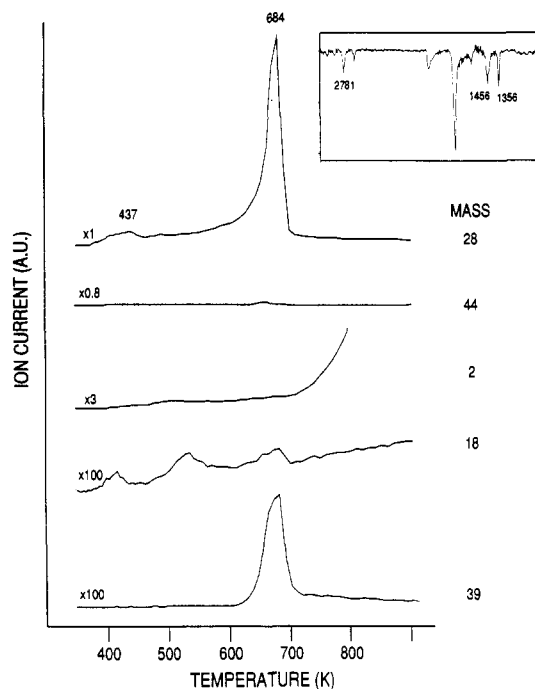


Figure 11. Postreaction thermal desorption mass spectra obtained after reaction of CO/H₂ with a $\sqrt{3}\times\sqrt{3}$ -R30°-K-Ru(001) surface at 550 K (2 Torr of CO + 13 Torr of H₂). (Heating rate: 5 K/s). The inset shows the vibrational spectrum obtained after quenching the reaction and evacuation of the high-pressure cell.

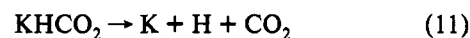
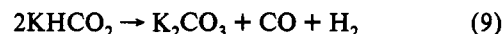
at 550 K followed by quenching to 300 K and evacuation to $<10^{-9}$ Torr. This procedure resulted in the vibrational spectrum shown in the inset of Figure 11, which shows that the layer consists of approximately equal amounts of formate (bands at 2781, 1356, and 760 cm^{-1} , $\theta \approx 0.15$), carbonate (1456 cm^{-1} , $\theta \approx 0.15$), CO coadsorbed with potassium (1764 cm^{-1} , $\theta \approx 0.15$), and CO adsorbed on the potassium-free Ru surface (1994 cm^{-1} , $\theta < 0.03$). The thermal desorption spectra in Figure 11 of mass 28 (CO), 44 (CO₂), 2 (H₂), 18 (H₂O), and 39 (K) are scaled according to their sensitivities as determined from a previous calibration.¹⁵ The major desorption features are due to CO and K, which desorb simultaneously at 684 K. Neither H₂ nor CO₂ show any significant desorption from the surface layer. (The large desorption of H₂ for $T > 700$ K results from the warming of the crystal mount or manipulator tube and is commonly observed after exposure to hydrogen at high pressure.) The absence of any significant desorption of CO₂ and H₂ below 700 K indicates that the formate decomposes mainly via C–O bond breaking to CO + OH. The C–H bond-breaking channel, which yields CO₂ + H, is not observed. A similar decomposition behavior has been observed in UHV model studies,¹⁵ where a pronounced shift in the decomposition pathway of the formate was found in the presence of potassium. On *clean* Ru(001), the C–H and C–O bond cleavage reactions occur simultaneously, leading to the production of equal amounts of CO and CO₂. In the presence of potassium, the C–H bond cleavage channel is suppressed, leaving CO and OH as the main decomposition products. The reaction of OH with K leading to KOH compound formation is thought to be the driving force for the preference of this reaction pathway.¹⁵ We note that in the present experiments the intensity of mass 18 (H₂O) is relatively weak, in contrast to the UHV model studies, where mass 18 was observed with higher intensity. This apparent discrepancy is due to difficulties in calibrating the sensitivity of mass 18. As discussed earlier, the pumping speed for H₂O in the drift tube of the mass spectrometer was found to vary strongly after repeated TDMS experiments thus frustrating attempts to calibrate the sensitivity of H₂O.¹⁵

The simultaneous desorption of CO and K at 684 K in Figure 11 demonstrates that the potassium is stabilized on the surface

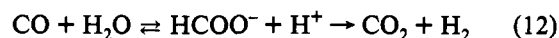
either by direct interaction with CO or by compound formation. When individually adsorbed, both K and CO desorb below 500 K. Previous UHV studies have shown that the direct attractive interactions between CO and potassium on the Ru(001) surface result in the mutual stabilization of both CO and K, far above the desorption temperature of the individual species.¹⁷ A similar effect, either as a result of direct interaction or compound formation, has been observed for a range of molecules. This observation is significant for catalytic reactions, since it demonstrates the thermal stability of a potassium layer in the monolayer coverage range at elevated reaction temperatures.

Formate Hydrogenation or Decomposition? The data presented above demonstrate the high reactivity of formate and the facile interconversion between potassium formate and carbonate. Two mechanisms can be invoked to explain the data—(1) *formate decomposition* in equilibrium with its formation and (2) *formate hydrogenation* to products such as methanol.

The *decomposition of the formate* can occur through several channels



Reaction 9 is the reverse of the formate synthesis reaction (6) and is the preferred pathway to potassium carbonate. Reaction 10 is the dominating decomposition channel under UHV conditions, as discussed earlier. Reaction 11 has been observed in the decomposition of formate on Ru(001) under UHV conditions, but *only in the absence of potassium*. However, this reaction is thought to be the dominant mechanism in the alkali-promoted water gas shift reaction over potassium-promoted Al₂O₃.³⁷



A mechanism for the *hydrogenation of the formate* can be proposed with the reaction



or



This mechanism provides at the same time a facile route to carbonate and thus is consistent with the reaction data shown for excess hydrogen in Figure 8. Since this mechanism produces either methane, (13), or methanol, (14), in the gas phase, the measurement of products must be the ultimate proof for this mechanism.

In order to pursue these questions further, GC and IR measurements of reaction products were performed at 10 Torr of CO + 40 Torr of H₂ and reaction temperatures from 450 to 600 K. Reaction of CO/H₂ with a potassium-free *clean* Ru(001) surface resulted in the formation of *methane* as the only product with rates corresponding to a turnover number of 0.2 molecules site⁻¹ s⁻¹ at 600 K. These rates were found to be in good agreement with previously published data for Ru(001) by Kelley and Goodman.⁴⁷ We find further that reaction over K–Ru(001) surfaces with *low coverage of potassium* ($\theta_{\text{K}} < 0.15$) resulted in a decrease of the methane formation rate and an increase in ethane production. The decrease in the total activity for alkane production was found to correspond to the loss of potassium-free ruthenium sites. A similar behavior had been reported previously for nickel by Campbell and Goodman⁷ and for iron by Wesner et al.⁶ and Dwyer.⁸ The measurement of the CO/H₂ reaction over a $\sqrt{3}\times\sqrt{3}$ -R30°-K-Ru(001) surface at 10 Torr of CO and 40 Torr of H₂ and temperatures from 450 to 600 K did not produce any evidence for significant amounts of methane or other alkanes exceeding our sensitivity level (TOF $> 10^{-4}$ molecules/(site s)). Likewise, we did not detect measurable amounts of methanol or

higher alcohols (with GC measurements). In this case, however, the detection sensitivity was significantly reduced by 2–3 orders of magnitude. GC test measurements showed that significant amounts of methanol were pumped by the stainless steel walls of the reactor and the GC tubing. Consequently, in the present work no further efforts were made to measure the production of alcohols. Future work has to show whether our failure to detect alkanes or alcohols in this reaction is due to a lack of sensitivity or due to low reactivity. It is known from methanol synthesis studies over Cu/ZnO/Al₂O₃ at high pressure that the hydrogenation of formate is the rate-limiting step⁹ and that the rate of the reaction obeys a first-order dependence in total pressure (H₂ + CO + CO₂) on copper below 1 atm.⁴⁸ The difficulties to measure products in the synthesis of alcohols over unpromoted single-crystal surfaces of copper have been well documented in the recent literature. Campbell et al.⁴⁹ performed methanol synthesis studies over Cu/ZnO(0001) and ZnO/Cu(111) single-crystal catalysts but were not able to detect methanol with GC measurements and estimated for the latter catalyst a TOF <2 × 10⁻³ molecules site⁻¹ s⁻¹ at 500–600 K and pressures up to 1500 Torr of CO + H₂. Szanyi and Goodman were able to measure methanol from the synthesis of CO₂/CO/H₂ on Cu(100) but found a TOF of 1.3 × 10⁻⁷ molecules site⁻¹ s⁻¹ at 525 K and 750 Torr pressure.⁴⁸ Finally, Taylor et al. have studied the hydrogenation of CO₂ over Cu(100) in the pressure range 0.5–5 atm.^{50,51} They report a synthesis rate for formate of 4.8 × 10⁻⁴ molecules site⁻¹ s⁻¹ at 363 K and a TOF of ≈10⁻² molecules site⁻¹ s⁻¹ for the further hydrogenation of the formate in H₂ at 6 atm and 363 K. However, in the latter study the hydrogenation of formate is inferred from the decrease of formate coverage after reaction in hydrogen, and no products (methanol or formic acid) were observed. From our data we obtain for CO/H₂ on the √3x√3-R30°-K-Ru(001) surface a rate of (1–3) × 10⁻³ molecules site⁻¹ s⁻¹ for the synthesis of formate from carbonate at temperatures of 450–500 K and pressures of 3–50 Torr. Assuming that hydrogenation is the rate-limiting step in the synthesis of methanol and that the reaction has a first-order dependence with pressure, the methanol synthesis rate may well be below our present detection limit.

D. Summary

Utilizing in-situ FT-IRAS we have characterized potassium-promoted Ru(001) surfaces under CO hydrogenation conditions, i.e., at 400–600 K and 1–50 Torr of CO/H₂.

1. Interaction of the √3x√3-R30°-K-Ru(001) surface with CO at 300 K and elevated pressure resulted in the formation of carbonate, which hydrogenated to formate after introduction of hydrogen via the reaction K₂CO₃ + CO + H₂ ⇌ 2KHCO₂. Characteristic vibrational features show that both formate and carbonate are *directly bound to the potassium*. This compound formation leads to a contraction of the potassium layer and *island formation* with the appearance of potassium-free domains on the Ru(001) surface.

2. Time-resolved FT-IRAS determined the *initial* rate of formate synthesis from carbonate to (1.7 ± 0.8) × 10⁻³ molecules site⁻¹ s⁻¹ at 500 K and 3 Torr of CO + H₂ (1:2). Isotope transient measurements result in a comparable synthesis rate under *equilibrium* conditions and hence demonstrate the reactivity of the formate. The surface formate and carbonate appear to be equilibrated at a *moderate CO/H₂ ratio*. The position of the equilibrium depends on temperature and partial pressures of the CO and H₂. Formate is formed at *low temperature and in the presence of both CO and H₂*. Entropy and mass action considerations suggest that the *decomposition* of formate → carbonate + CO + H₂ will be favored at *high temperature and low partial pressures* of CO or H₂.

3. The formate observed under reaction conditions was shown to be more stable than analogue model compounds produced under

UHV conditions. This enhanced stability is due to two factors: (i) Compound formation with potassium stabilizes the formate relative to formate adsorbed on the potassium-free ruthenium substrate and (ii) coadsorption of CO next to the formate ($\nu_{\text{CO}} \approx 1750 \text{ cm}^{-1}$). The presence of coadsorbed CO was found to depend on the composition of the reaction gas CO and H₂.

The results demonstrate for the CO hydrogenation reaction at high potassium coverage a dual promoter mechanism—(i) promotion of CO dissociation resulting in the formation of carbonate and (ii) direct participation in the synthesis of formate via compound formation.

Acknowledgment. We are grateful to C. T. Campbell, I. Chorkendorff, and A. Wokaun for sending us manuscripts of their work prior to publication.

References and Notes

- (1) Bonzel, H. P. *Surf. Sci. Rep.* **1987**, *8*, 43 and references therein.
- (2) Ertl, G.; Weiss, M.; Lee, S. B. *Chem. Phys. Lett.* **1979**, *60*, 391.
- (3) Strongin, D. R.; Somorjai, G. A. *J. Cat.* **1988**, *109*, 51.
- (4) Paul, J.; de Paola, R. A.; Hoffmann, F. M. *Physics and Chemistry of Alkali Adsorption*. In *Materials Science Monographs*; Bonzel, H. P., Bradshaw, A. M., Ertl, G., Eds.; Elsevier: New York, 1989; Vol. 57; p 213 and references therein.
- (5) Broden, G.; Gafner, G.; Bonzel, H. P. *Surf. Sci.* **1979**, *84*, 295. Bonzel, H. P.; Broden, G.; Krebs, H. J. *Appl. Surf. Sci.* **1983**, *16*, 373.
- (6) Wesner, D. A.; Coenen, F. P.; Bonzel, H. P. *Langmuir* **1985**, *1*, 478.
- (7) Campbell, C. T.; Goodman, D. W. *Surf. Sci.* **1982**, *123*, 413.
- (8) Dwyer, D. J. *Physics and Chemistry of Alkali Adsorption. Materials Science Monographs*; Bonzel, H. P., Bradshaw, A. M., Ertl, G., Eds.; Elsevier: New York, 1989; Vol. 57; p 307.
- (9) Klier, K.; Herman, R. G.; Nunan, J. G.; Smith, K. J.; Bogdan, C. E.; Young, C. W.; Santiesteban, J. G. *Methane Conversion*; Bibby, D. M., Chang, C. D., Howe, S., Yurchak, R. F., Eds.; Elsevier: New York, 1988; p 109 and references therein.
- (10) Sheffer, G. R.; King, T. S. *J. Catal.* **1989**, *115*, 376.
- (11) (a) Hoffmann, F. M.; Robbins, J. L. *J. Electron Spectrosc. Relat. Phenom.* **1987**, *45*, 421. (b) *Proc. 9th Int. Congr. Catal.* Calgary; 1988; p 1144.
- (12) Hoffmann, F. M. *J. Chem. Phys.* **1989**, *90*, 2816.
- (13) Pfnür, H.; Hoffmann, F. M.; Ortega, A.; Menzel, D.; Bradshaw, A. M. *Surf. Sci.* **1980**, *93*, 431.
- (14) De Paola, R. A.; Hrbek, J.; Hoffmann, F. M. *J. Chem. Phys.* **1985**, *82*, 2484.
- (15) Weisel, M. D.; Chen, J. G.; Hoffmann, F. M.; Sun, Y. K.; Weinberg, W. H. *J. Chem. Phys.* **1992**, *97*, 9396.
- (16) Note that the intensity of the gas-phase band of CO is not linear with CO pressure. The long optical pathlength and the narrow linewidth of gas-phase CO (not resolved here) lead to line saturation and hence nonlinearity of the band intensity with pressure.
- (17) Hoffmann, F. M.; Hrbek, J.; de Paola, R. A. *Chem. Phys. Lett.* **1984**, *106*, 83.
- (18) Weisel, M. D.; Hoffmann, F. M.; Paul, J. To be submitted.
- (19) Hoffmann, F. M.; Weisel, M. D.; Fu, Z.; Eberhardt, W. E.; Stevens, P.; Paul, J. In preparation.
- (20) Paul, J.; Hoffmann, F. M. *Catal. Lett.* **1988**, *1*, 445.
- (21) Paul, J. *Surf. Sci.* **1989**, *224*, 348.
- (22) Liu, Z. M.; Zhou, Y.; Solymosi, F.; White, J. M. *J. Phys. Chem.* **1989**, *93*, 4383.
- (23) Wohlrab, S.; Ehrlich, D.; Wambach, J.; Kuhlbeck, H.; Freund, H.-J. *Surf. Sci.* **1989**, *220*, 243.
- (24) Paul, J.; Hoffmann, F. M.; Robbins, J. L. *J. Phys. Chem.* **1988**, *92*, 6967 and references therein.
- (25) Wyckoff, R. W. G. *Crystal Structures*, 2nd ed.; Wiley Interscience Publ.: New York, 1963; Vol. 1.
- (26) Gatehouse, B. M.; Lloyd, D. J. *J. Chem. Soc. Dalton Trans.* **1973**, 70.
- (27) Bats, J. W.; Fuess, H. *Acta Crystallogr.* **1980**, *B36*, 1940.
- (28) Weisel, M. D.; Chen, J. G.; Hoffmann, F. M. *J. Electron Spectrosc. Relat. Phenom.* **1990**, *54/55*, 787.
- (29) Ito, K.; Bernstein, H. J. *Can. J. Chem.* **1956**, *34*, 1970.
- (30) Kantschewa, M.; Albano, E. V.; Ertl, G.; Knözinger, H. *Appl. Catal.* **1983**, *8*, 71.
- (31) Koepfel, R. A.; Baiker, A.; Schild, C.; Wokaun, A. *J. Chem. Soc., Faraday Trans.* **1991**, *87*, 2821.
- (32) Avery, N. R.; Toby, B. H.; Anton, A. B.; Weinberg, W. H. *Surf. Sci.* **1982**, *122*, L574.
- (33) Bats, J. W.; Fuess, H. *Acta Crystallogr.* **1980**, *B36*, 1940.
- (34) de Paola, R. A.; Hoffmann, F. M. Unpublished data.
- (35) Weisel, M. D.; Hoffmann, F. M.; Robbins, J. L. Unpublished data.
- (36) Berthelot, M. *Ann. Chim. Phys.* **VIII 1906**, *9*, 174.
- (37) Amenomiya, Y.; Pleizier, G. *J. Catal.* **1982**, *76*, 345.
- (38) Dalla Betta, R. A.; Shelef, M. A. *J. Catal.* **1978**, *48*, 111.

(39) Solymosi, F.; Erdöhelyi A.; Kocsis, M. *J. Chem. Soc., Faraday Trans.* **1981**, *77*, 1003.

(40) Robbins, J. L.; Marucchi-Soos, E. *J. Phys. Chem.* **1989**, *93*, 2885.

(41) The nonlinearity of the IR intensity at high coverage results from the vibrational depolarization of neighboring molecules as discussed in detail for CO/Ru(001).⁴² The latter example shows that the IR intensity of the C–O stretch at 2000 cm⁻¹ exhibits linear behavior only at low coverage. It becomes increasingly nonlinear at higher coverage ($\theta_{\text{CO}} > 0.20$), and at $\theta_{\text{CO}} = 0.33$ the dynamic dipole moment has decreased to approximately 50% of the zero coverage value. It is reasonable to assume that the formate $\nu(\text{CO})_s$ mode exhibits a similar or weaker nonlinearity in view of the comparable dynamic dipole moments for the C–O stretches of these two molecules. Based on this analogy we conclude that the nonlinearity of the dipole moment is not important at low coverage but introduces an error at high formate coverage ($\theta > 0.2$).

(42) Hoffmann, F. M. *Surf. Sci. Rep.* **1983**, *3*, 107.

(43) Isotopic transient measurements are usually performed in flow experiments by *switching* of the isotopic label. In batch reactors the isotopic label has to be introduced by the *addition* of gas. The latter method was

employed in the present experiment. In order to ensure that the addition of the isotopic label did not result in a nonequilibrium situation, the pressure conditions were chosen such that the increase of CO pressure by the addition of CO* did not result in a change of the formate coverage.

(44) For details on the calculations, see ref 15.

(45) Hoffmann, F. M.; Weisel, M. D. *Surf. Sci.* **1992**, *269/270*, 495.

(46) We note that in this case carbonate is *not* observed. Since we were not able to identify the decomposition (or reaction) products, it is not clear whether the formate decomposes (eq 6) or hydrogenates (eqs 13, 14) as a result of the high partial pressure of hydrogen.

(47) Kelley, R. D.; Goodman, D. W. *Surf. Sci.* **1982**, *123*, L743.

(48) Szanyi, J.; Goodman, D. W. *Catal. Lett.* **1991**, *10*, 383.

(49) Campbell, C. T.; Daube, K. A.; White, J. M. *Surf. Sci.* **1987**, *182*, 4587.

(50) Taylor, P. A.; Rasmussen, P. B.; Ovesen, C. V.; Stoltze, P.; Chorkendorff, I. *Surf. Sci.* **1992**, *261*, 191.

(51) Chorkendorff, I.; Taylor, P. A.; Rasmussen, P. B. *J. Vac. Sci. Technol.* **1992**, *A10*, 2277.